Environmental Science Nano

Prolonging the antibacterial activity of nanosilver-coated membranes through partial sulfidation

Journal:	*Environmental Science: Nano*
Manuscript ID	EN-ART-03-2020-000300.R2
Article Type:	Paper

Prolonging the antibacterial activity of nanosilver-coated membranes through partial sulfidation

Ana C. Barrios[1,2], Dianne Carrillo[1,2], Tyson R. Waag[1,2], Douglas Rice[1,2], Yuqiang Bi[1,2], Rafiqul Islam[3], and François Perreault[1,2]*

[1] School of Sustainable Engineering and the Built Environment, Arizona State University

[2] Nanosystems Engineering Research Center for Nanotechnology-Enabled Water Treatment, Arizona State University, Tempe, Arizona, United States

[3] Cactus Materials Inc., Tempe, Arizona, United States

* Corresponding Author: Francois Perreault, francois.perreault@asu.edu

Submitted to:

Environmental Sciences: Nano

* Corresponding Authors: Francois Perreault, Email: francois.perreault@asu.edu, Phone: (480) 965-4028. Mailing address: College Avenue Commons (CAVC) Building, 660 S. College Avenue, #507, Tempe, AZ 85281, USA.

Abstract

Biofouling is a major issue in membrane-based water treatment because it shortens membrane life and decreases the permeate flux. Silver, a known biocide, is often used for *in situ* formation of silver nanoparticles (Ag NPs) on membranes for biofouling mitigation. However, Ag NPs dissolve quickly in water, limiting their effectiveness over long periods of time. This study focuses on the modification of silver-functionalized reverse osmosis (RO) membranes with different concentrations of Na_2S (10^{-1}, 10^{-3}, and 10^{-5} M) to identify the degree of sulfidation that limits Ag release while preserving the antibacterial effect. Sulfidized membranes decreased Ag release by > 85% depending on the extent of sulfidation. Antibacterial activity was assessed using *P. aeruginosa* and *E. coli*. Results showed the highest inactivation at 73% for *P. aeruginosa* and 57% for *E. coli* for 10^{-5} and 10^{-3} M Na_2S-treated membranes, respectively, while the more sulfidized membrane treated with 10^{-1}M Na_2S treatment had the lowest antibacterial effect. Moreover, when tested in a dynamic cross-flow RO system for 24h, the flux declined by 24% for the Ag NPs and by 23%, 17%, and 19% as the extent of sulfidation increased. Additionally, the Ag remaining in the membrane was higher for the highest sulfidized membrane with 519 ng/cm^2. Therefore, retention of the silver coating over time appears to be more important for biofilm control in RO systems than high antibacterial activity. Both 10^{-5} M and 10^{-3} M Na_2S-treated membranes had the best balance between reduced dissolution rate and good antibacterial and anti-biofouling performance, respectively.

Environmental significance:

While the antibacterial activity of silver nanoparticles is widely attributed to the release of silver ions, their rapid release prevents the efficient application of Ag NPs on surfaces. One of such applications is in water treatment, where Ag NPs have been successfully functionalized onto membrane modules for biofilm reduction; however, their short-lived attachment limits the NPs usability. Here, we examine a functionalization technique that significantly slows down silver ion release through sulfidation of Ag NPs on reverse osmosis membranes. Sulfidation prolongs the antibacterial activity of the membrane while maintaining its integrity and functionality. This strategic design suggests that sulfidation is a promising technique to optimize silver usage and reduce its release in the environment.

1. Introduction

Each year, 2.7 billion people face severe water scarcity for at least one month per year. This dearth of freshwater arises from the rising demand driven by a growing global population and expanding international economies, as well as decreases in supply due to over-exploitation of resources and climate change.[1] To bridge the gap between freshwater supply and demand, many utilities are investing in desalination to tap into alternative water sources such as seawater, brackish groundwater, and wastewater.[2,3] Reverse osmosis (RO) is the state-of-the-art technology for desalinating water. RO is a membrane-based process that is more energy-efficient than other thermal desalination systems.[4] However, desalination by RO is still limited by considerable economic and environmental costs, both of which must be mitigated to ensure the sustainability of this increasingly vital water treatment process.

Biofouling, or the attachment and proliferation of microorganisms on a surface, reduces the efficiency of RO and contributes to the high economic and environmental costs of operating RO systems. The formation of biofilms, a heterogeneous assembly of microbial cells and extrapolymeric substances (EPS), on membranes increases the hydraulic resistance in the membrane module, resulting in higher energy requirements to maintain a constant transmembrane pressure differential.[5,6] Moreover, biofilm-enhanced osmotic pressure at the membrane interface can negatively impact the quality of the permeate.[7] To mitigate the effects of biofouling, operators must conduct extensive chemical cleaning procedures, which add to the operational expenses, damage membranes, and cause downtime in water production.[8,9] Altogether, the direct and indirect impacts of fouling, from increased energy usage to chemical and operational expenses associated with feed water pre-treatment and membrane cleaning, leads to significant economic impacts, with previous work estimating from 25 to up to 50% of the plant's total operating costs.[8,10]

For over a decade, research efforts have been made to design membranes resistant to biofouling.[11,12] One strategy involves imparting biocidal properties to membrane surfaces in an effort to reduce deposition, attachment, and adhesion of bacteria or inhibit their proliferation.[13,14] Membranes functionalized with biocidal materials such as graphene oxide, copper, selenium, or antibacterial polymer brushes have been shown to outperform control membranes in terms of flux decline and biofilm formation.[15–18] The most commonly used antibacterial compound for biofouling control is silver [19–26]. In its ionic form, silver is a strong antibacterial compound that inactivates cells through several pathways, including cell lysis and DNA damage.[27] Although a particle-mediated effect is generally acknowledged[28,29], the current paradigm for the antibacterial action of Ag NPs is that it is primarily driven by its capacity to release free silver ions, which is mediated by the presence of oxygen in the water.[30,31] Previous studies have shown that Ag NPs made insoluble through surface coatings on Ag NP surfaces have considerably reduced antibacterial properties.[31–33] Therefore, the focus of silver-based coatings for biofouling

control has been on the more soluble zerovalent form of silver, either as Ag NPs or Ag NPs composites.[19–22,24,34,35]

However, the high solubility of zerovalent Ag NPs under aerobic conditions poses challenges for its implementation in water treatment systems. The fast release of silver ions from nanoparticles' coatings leads to a rapid loss of antibacterial performance over time in silver-coated membranes.[19,36] A Goldilocks conundrum thus arises, as silver must be released into its ionic form at a rate fast enough to drive concentrations to biocidal levels, but not so rapidly that the silver coating is depleted early in the membrane's life-cycle. Recent studies have proposed different approaches to prolong the antibacterial life of the silver coating on membranes. Higher silver loadings have been applied to membranes using layer-by-layer coating methods.[19] Slower release rates have been achieved using silver composites such as silver-loaded zeolites,[26] through mussel-inspired polydopamine chemistry,[35–37] or by embedding the particles into the polyamide layer of the membrane.[38] However, these chemistries can be complex or expensive, which may limit the applicability for commercial implementation.

In this report, we describe a simple and inexpensive surface modification procedure to generate a slow-release silver-based biocidal coating on RO membranes. Membranes coated with Ag NPs were partially sulfidized to Ag_2S to slow down the release of silver. Static and dynamic biofouling assays reveal that although a balance exists between antibacterial activity and silver solubility, slower release rate and higher silver longevity on the membrane are more important for dynamic conditions in membrane systems. These results provide important guidelines for the design of more cost-efficient silver-based antibacterial coatings.

2. Materials and Methods

2.1 Materials

All chemicals and supplies were obtained from Sigma-Aldrich (Saint Louis, MO), except as noted below, and were of ACS grade or higher. Sodium borohydride powder was obtained from Acros Organics (New Jersey). A Dow FILMTEC™ BW30 membrane (Midland, MI) was used for all experiments. The bench scale RO module was constructed using Swagelok (Salon, OH) materials. Unless specified, all the solutions were prepared in deionized (DI) water from a GenPure UV xCAD plus ultrapure water purification system (Thermo Scientific, Waltham, MA).

2.2 Membrane modification

2.2.1 *In situ* formation of Ag NPs

Membrane modification was done following a protocol adapted from Ben-Sasson et al.[22] First, dried polysulfone RO membranes were wetted through immersion in 20% isopropanol and 80% DI water for 20 min. Then, the membranes were rinsed and soaked

three times in DI water. These unfunctionalized, washed membranes were used as controls. The *in situ* formation of Ag NPs on the RO membranes was carried out as described below. The active layer of the membrane was placed in between a glass plate and a plastic frame (hole size 7.5 cm x 12 cm) to hold the solutions used for the modification. First, 50 mL of a 3 mM $AgNO_3$ solution was added to the active layer of the membrane for 10 min and agitated. Then, the $AgNO_3$ solution was discarded, leaving the active layer with a thin film of adsorbed solution wetting the surface. Next, 50 mL of a 3 mM $NaBH_4$ solution was added for 5 min to form silver nanoparticles on the membrane surface. The solution was then discarded. Finally, the membrane was rinsed with 10 mL of DI water for 10 s to remove excess reagents. All *in situ* reactions were done at room temperature.

2.2.2 Sulfidation of Ag NPs

The previously prepared Ag NP membrane was sulfidized following the protocol by Levard et al.[32] Following the procedures described in 2.2.1, the membranes were kept in the frames and Ag NPs were sulfidized by adding 50 mL of either a 10^{-5}, 10^{-3}, or a 10^{-1} M sodium sulfide (Na_2S) solution, prepared in a 0.01 M $NaNO_3$ electrolyte, to the membrane surface. The membranes were agitated with the reagents for 24h at room temperature, rinsed with DI water and stored in a closed container until used. The solutions were prepared fresh for each experiment.

2.3 Membrane characterization

Contact angles (CA) were taken on an Attension Theta by Biolin Scientific (Gothenburg, Sweden) using a 1001 TPLT Hamilton syringe (Reno, NV). To account for variability, at least 5 different CA measurements, from different areas of the membrane, were taken per sample. For each measurement, the software recorded ~200 data points over 10s. The CA values were averaged and reported as a final mean and displayed as average ± standard deviation. X-ray photoelectron spectroscopy (XPS) was done on a VG 220i-XL (Thermo Fisher Scientific Ltd. Hampton, NH) equipped with a monochromated Al K-alpha X-ray source. The data was analyzed using the CasaXPS software (version 2.3.18). Membrane surface roughness was analyzed by atomic force microscopy (AFM). AFM was performed using tapping mode with a Bruker Multimode 8 AFM (Digital Instruments, Plainview, NY) equipped with an NCHV (Bruker, Camarillo, CA.

Surface zeta potential was evaluated for each experimental membrane utilizing streaming potential measurements with a ZetaCAD analyzer incorporating a flat surface cell (CAD Instruments, Les Essartes-le-Roi, France) with a 0.1 mm spacer to create a stable opening during testing. An electrolyte solution comprised of 5 mM KCl and 0.1 mM HCO_3 was used throughout the analysis and measurements were taken over a pH range from 4-10, with a pressure range from 30-70 psi, and step durations of 30 and 60 seconds to determine the zeta potential of each membrane.

Membrane morphology was evaluated using scanning electron microscopy (ESEM-FEG XL-30, Philips Hitachi SU-70, Hillsboro, OR) at an acceleration voltage of 10 kV. Transmission electron microscopy (TEM) was performed on unsulfidized and sulfidized (10^{-1}M Na_2S) membranes. High and low-resolution TEM images were obtained by a JEOL 2010F coupled with an Energy Dispersive X-ray (EDX) detector for species determination at an accelerating voltage of 200 kV equipped with a CCD camera. TEM samples were prepared using the focused ion beam (FIB) FEI Nova 200 Nanolab with a Ga^+ ion beam from the Eyring Materials Center at ASU. Briefly, the membranes were placed on a SEM stub and held in place with copper tape. Then, they were carbon-coated before putting them in the FIB. An initial protective layer of Pt was deposited with an electron beam, followed by another Pt layer deposited with the ion beam. All ion beam work was done at 30 kV except for the final cleaning, which was done at 5 kV.

The transport properties of the membrane were examined in a dead-end filtration system. Each membrane type was cut in circles with a 5 cm diameter. First, the membranes were rinsed with 20% isopropyl alcohol for 20 min then in Nanopure water (Barnstead™, Thermo Fisher Scientific) for 20 min before placing it in the dead-end cell. The system was completely closed, and the membranes were compacted at 300 psi for 1hr. An aliquot was collected every 15 min and weighed with a balance to determine the flux. After compaction, the system was opened and a 2000 mg/L NaCl solution was used to assess salt rejection. Salt concentration was measured using a COM-100 HM digital conductivity meter.

2.4 Quantification of silver leaching

Bench-scale batch tests were done to quantify silver release from the functionalized RO membranes. Following the protocol by Bi et al.,[39] three circular membrane coupons (⌀ = 2.5 cm, A=4.9 cm^2), from different membranes and for each membrane type were placed in 40 mL of extraction solution (deionized water) in individual 50 mL Falcon tubes and agitated continuously using a benchtop orbital shaker (Branstead Lab-Line, 80 rpm). Silver release was done at different time points: 0, 30, 60, 180, and 360 min. For each time point, the agitation was stopped, and the membranes were removed from the extraction solution. The leachates were then analyzed for silver content using Inductively Coupled Plasma-Mass Spectroscopy (ICP-MS, Thermo Scientific X Series II). The membrane was then acid digested by 10% trace metal grade HNO_3 to quantify residual Ag. The batch tests were done in triplicates at each time point. The release rate was calculated using the silver content remaining on the membrane after acid digestion in each time point mentioned above; the slope of the line was used as the release rate.

2.5 Antibacterial properties of functionalized membranes

Pseudomonas aeruginosa (*P. aeruginosa*, ATCC 15692) and *Escherichia coli* (*E. coli*, W3110, ATCC 27325) were obtained from the American Type Culture Collection. Cultures were maintained on Lysogeny Broth (LB) agar plates stored at 4ºC and

manipulated using aseptic techniques to avoid contamination. For both *E. coli* and *P. aeruginosa*, the purity of the culture was verified using the Brilliance™ and Cetrimide agar selective media, respectively. Antibacterial properties on the pristine and functionalized membranes were assessed using a colony forming unit (CFU) assay. Before the experiments, all glassware, solutions and materials required were autoclaved for proper sterilization. Proper personal protective equipment was worn, and all the experiments were done in a biosafety cabinet under sterile conditions. Circular membrane coupons of 2.5 cm in diameter were punched and placed in plastic holders leaving the active site exposed. For each culture, a colony was selected from a plate streak prepared with either fresh *E. coli* or *P. aeruginosa* stocks (kept at 4° C) grown overnight in 25 mL of Lysogeny Broth (LB) in an Isotemp incubator (Fischer Scientific) at 37°C and placed on a shaker at 140 rpm. The cultures were then diluted in fresh LB (1:25) and cultivated in the same conditions until the optical density (OD) reached 1.0 at 600 nm. Aliquots of bacterial cells were taken and washed 3 times by centrifugation and resuspended in 0.9% NaCl to remove any cell debris. A 3 mL aliquot of the bacterial suspension (10^7 CFU/mL in 0.9% NaCl) was contacted with the membrane's active layer for 3h at room temperature. The suspension was discarded, and the membranes were washed with 0.9% NaCl to remove non-adhered cells. The coupons were placed in 50 mL falcon tubes containing 10 mL of 0.9% NaCl and bath sonicated for 10 minutes to detach bacteria from the surface. For the plating assays, 100 µL of the sonicated solution were withdrawn and diluted with 900 µL of fresh autoclaved 0.9% NaCl in Eppendorf tubes. The solution was vortexed and a 50 µL aliquot was collected and plated in an LB agar plate and incubated overnight. The CFU counts were done the next day and results were normalized with respect to the control CFU value.

2.6 Bench-scale RO biofouling

Dynamic biofouling experiments were executed utilizing a bench-scale cross flow RO system with a three-cell configuration and a 15 L volume of synthetic secondary wastewater effluent (ionic strength of 15.9 mM) as feed water.[40] The composition and concentration of the synthetic secondary wastewater is as follows: NaCl at 468 mg/L, $MgSO_4 \cdot 7H_2O$ at 37 mg/L, $NaHCO_3$ at 42 mg/L, $CaCl_2 \cdot 2H_2O$ at 29 mg/L, KH_2PO_4 at 35 mg/L, NH_4Cl at 21 mg/L, $Na_3C_6H_5O_7 \cdot 2H_2O$ at 176 mg/L, and glucose at 100 mg/L. The RO system was initially loaded with control (not functionalized) or silver-functionalized BW30 brackish membranes (Dow, Midland, MI), pre-wetted for 15 min in 50% isopropanol, with an active area of 38.64 cm^2 (8.4 cm × 4.6 cm). Cell one was used for the control, while cells two and three were used for the experimental membranes. Pressure, temperature, and cross flow were controlled at a constant 325 psi, 20 °C, and 37.8 cm/s, respectively. The permeate flux for each cell was measured continuously using Sensirion SLI-2000 flow meters (Staefa, Switzerland) and the collected flux data was compiled into rolling averages of 20 data points. For each experiment, the membranes were first compacted at 325 psi until the permeate flux reached a stable value (~4 h), after which the salts were added. *Pseudomonas aeruginosa* (*P. aeruginosa*, ATCC 15692) was used as a

model biofilm-forming organism. It was grown overnight in LB broth on a shaker plate at 140 rpm in an Isotemp incubator (Fisher Scientific) at 37°C. The culture was then diluted in fresh LB on a 2:25 ratio and grown in the same conditions until the OD reached 1.0 at 600 nm. The cells were then washed by centrifugation 3 times with the synthetic secondary wastewater. The bacteria were then diluted in that same medium at a 1:10 ratio. After a brief re-stabilization (~45 min), bacteria were added at a concentration of 2.5×10^6 cells/mL (50 mL) to induce biofouling of the membranes. Biofouling experiments were conducted for 24 h. After each experiment, the membranes were collected, briefly rinsed in DI water, and then digested by 10% HNO_3 to determine the amount of silver remaining on the membrane using ICP-MS.

2.7 Data analysis and statistics

All treatments were prepared in at least three independent replicates. To account for the inherent variability of both membrane surface chemistry and bacterial experiments,[41–45] antimicrobial assays were performed in triplicates and repeated in three independent experiments at a minimum (i.e. n=9). Means and standard deviations were estimated for each treatment and results were normalized with respect to the control. Data was assessed for normality using the Shapiro-Wilk test and all skewness and kurtosis z-values were well within the normal range of -1.96 to +1.96. Statistical differences between control samples (no Ag NPs) and silver-functionalized membranes, were determined via a one-way analysis of variance (ANOVA), followed by a Tukey post-hoc test where a p value less than 0.05 was considered significant. Statistical analysis was done using the Statistical Package for Social Sciences software (SPSS) version 26.

3. Results and Discussion

3.1 Sulfidized membranes characterization. The successful functionalization of the pristine membrane was confirmed by both SEM microscopy and XPS. The functionalization process was done in two stages: 1) *in situ* formation of Ag NPs on the RO membrane and 2) sulfidation of Ag NPs. The first stage only requires two reagents, silver nitrate and a reducing agent; the second stage requires a sulfidizing agent, in this case, sodium sulfide. In stage 1, $AgNO_3$ is added and eventually removed, leaving a thin film of solution covering the active layer of the membrane. The reducing agent is added to reduce the free Ag ions in the residual thin film, precipitating Ag NPs in the membrane surface. In stage 2, different concentrations of Na_2S were added so that the Ag NPs react with the inorganic sulfide in solution to from Ag:Ag_2S particles.[32]

Figure 1 displays SEM micrographs of the control membrane, the Ag NP functionalized membrane (stage 1 only) and the sulfidized membrane (stages 1 and 2). Based on these images (Figure 1a-c), all the surfaces show a "ridge and valley" structure characteristic of the polyamide layer.[24,46] Although the SEM micrographs show no significant visual difference between the control (A), Ag NP-modified (B), and sulfidized membranes (C), there is an evident color change from white to a dark yellow-brown color once the Ag NPs formed on the membrane's surface.[24] Subsequently, the color changed from yellow-brown to a dark brown after addition of the highest concentration of Na_2S.[47] The transformations from Ag NPs to Ag:Ag_2S NPs were further confirmed by TEM (Figure 1 panels D-G). These results indicate d-spacing values of 0.257 and 0.269 nm for Ag and Ag_2S, confirming the formation of Ag_2S at the surface of the Ag NPs as supported by other studies.[48–51] EDAX spectroscopy confirms the presence of Ag (2.98 keV) and sulfur (2.31 keV) for the sulfidized membrane.

XPS measurements were done to analyze the elemental composition of the functionalized membranes (Table 1). As expected, silver was not detected on the control membranes. The functionalized membranes kept a constant Ag content with an average of 7.78% Ag regardless of the extent of sulfidation. Additionally, XPS shows an increase of sulfur as the concentration of Na_2S increases. The other elements detected by XPS were carbon, oxygen, and nitrogen (peaks at 281, 396, and 527 eV for C 1s, N 1s, and O 1s, respectively), which appear in all the spectra (control and *in situ* modified membranes), as these elements are constituents of the polyamide layer. According to the surface elemental analysis, the nitrogen/carbon ratio at the membrane surface was slightly reduced for the *in situ* modified membranes. This reduction, likely due to masking of the polyamide amine group by the Ag NPs, indicates a decrease in the nitrogen coverage and implies that nitrogen (from the precursor $AgNO_3$ solution) had no significant content in the formed Ag-NPs.[22] The carbon/oxygen ratio on the membrane surface exhibited an increase from 0.80 to 1.1 for the control membrane and sulfidized membrane (10^{-1}M Na_2S), respectively, indicating a decrease in oxygen content. The decrease in C/O ratio may be associated with

the functionalization process, as oxygen functional groups are known to serve as anchor sites for nanoparticles during the heterogeneous nucleation process.[34,52,53] Therefore, it can be concluded that the *in situ* Ag NPs on the membrane comprised of metallic silver and Ag:Ag_2S NPs after sulfidation.

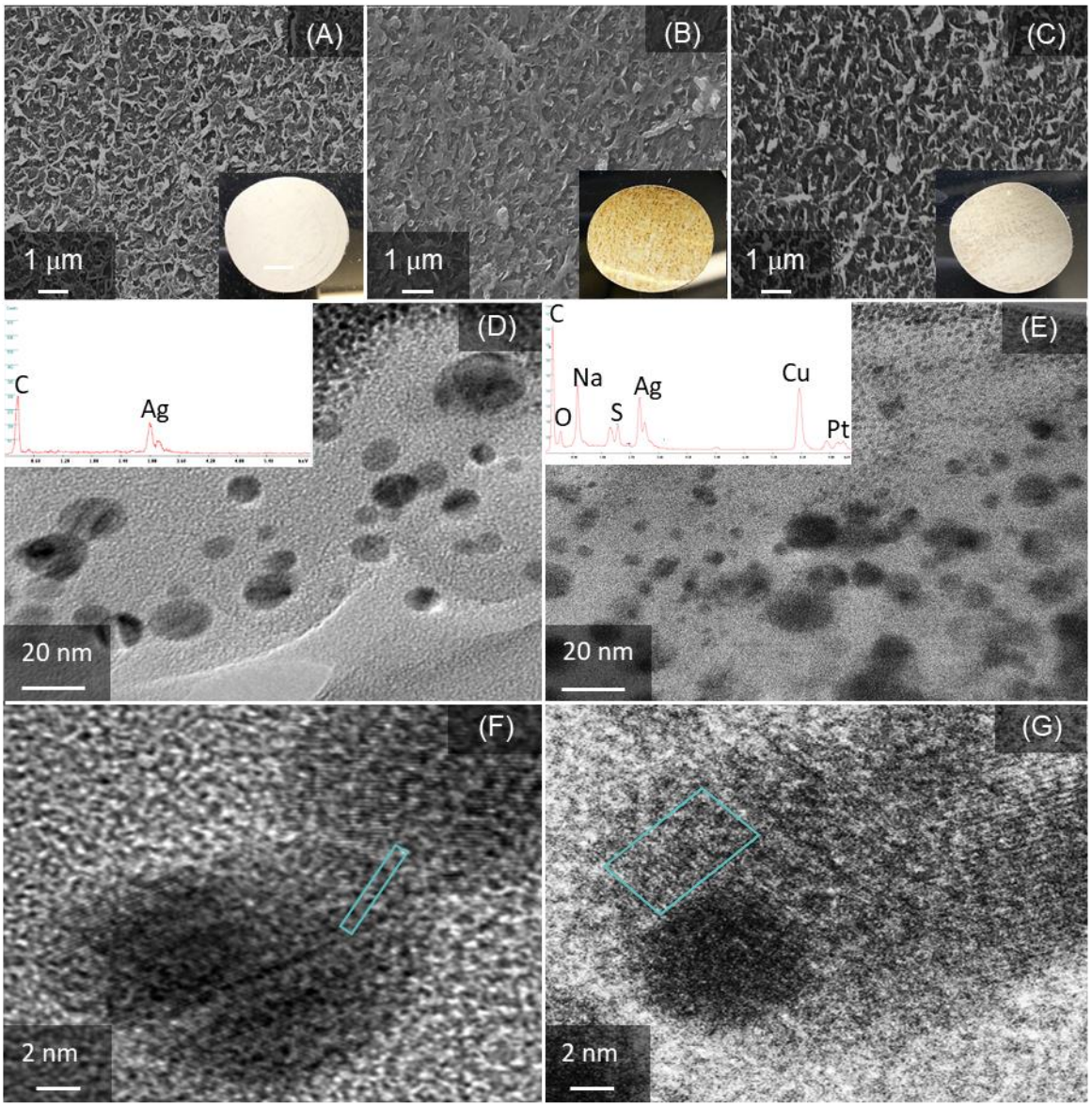

Figure 1. Sulfidized membranes characterization. Scanning electron microscopy imaging of A) control, B) Ag NPs functionalized, and C) sulfidized Ag NPs membranes. Inserts shows the visual change in the membrane surface. Solutions of 3 mM $AgNO_3$ and 3 mM $NaBH_4$ were used during the *in situ* formation reaction. Samples were sputter coated with gold and platinum and images were taken at 10 kV acceleration voltage. Low resolution TEM images of the polyamide active layer with D) Ag NPs and E) sulfidized Ag NPs. Inserts show EDAX spectra (in red) of each membrane. High resolution TEM images of

F) Ag NPs and G) sulfidized Ag NPs. A concentration of 10^{-1} M Na_2S was used to sulfidize the Ag NPs. The teal colored box represents the area where the fringe analysis was done.

Table 1. Compiled XPS data representing atomic percent of the carbon, oxygen, nitrogen, silver, and sulfur content for the pristine and functionalized membranes.

	% C 1s	% O 1 s	% N 1s	% Ag 3d	% S 2p
Control	42.3 ± 3.7	52.7 ± 3.0	5.1 ± 0.7	n.d.	n.d.
Ag NP	42.0 ± 4.3	49.2 ± 0.7	1.27 ± 1.39	6.95 ± 4.0	0.09 ± 0.8
10^{-5} M Na_2S	40.7 ± 3.0	50.5 ± 1.4	<0.5	7.49 ± 1.6	0.83 ± 0.2
10^{-3} M Na_2S	46.4 ± 2.8	43.7 ± 0.9	<0.5	8.34 ± 1.8	1.09 ± 0.4
10^{-1} M Na_2S	46.5 ± 2.9	43.8 ± 0.8	<0.5	8.35 ± 1.8	1.21 ± 0.5

3.2 Functionalization alters the surface properties of control membranes. Membrane surface properties such as roughness, permeability, or hydrophilicity will dictate the fouling propensity of the membrane.[2] As such, it is important to evaluate how functionalization may impact these surface properties compared to the control membrane. Results indicate that, except for the 10^{-3}M Na_2S treated membrane, modification significantly increased surface roughness compared to the control (Figure 2A). As determined by AFM, the control membrane had an average surface roughness of 22.9 nm ± 5.48, whereas the functionalized membranes had values of 49.0 nm ± 12.7 for Ag NPs, 53.6 nm ± 4.41 for 10^{-5} M Na_2S , 42.3 nm ± 17.6 for 10^{-3} M Na_2S, and 61.2 nm ± 16.6 for 10^{-1} M Na_2S. It is noteworthy that although there is no statistical difference between silver functionalized and sulfidized membranes, roughness tends to increase as the amount of Na_2S increases.

Surface wettability was assessed by measuring the water contact angle (CA). On one hand, functionalization with either Ag NPs or sulfidized Ag NPs did not impact the CA when compared to the control, which had a CA of 43.8° ± 12.8, similar to the findings of Ben-Sasson et al.[22] On the other, sulfidation of Ag NPs using all Na_2S concentrations (10^{-5} to 10^{-1}M) increased the hydrophilicity of the membranes compared to the Ag NPs, reducing the CA from 51.3° ± 3.56 to an average of 34.3° ± 7.98 for the sulfidized Ag NPs (Figure 2B). Surface charge, measured as the surface streaming potential, show a slight increase to less negative values after functionalization. However, these changes were not significant (Figure 2C).

RO systems usually require membranes with high salt rejection and high water permeability.[54] It has been previously reported that silver functionalization on RO membranes can decrease water permeability but has minimal impact on salt selectivity.[22]In this study, none of these parameters were affected even after the sulfidation of silver at different concentrations (Figure S1). Previous studies show that hydrophilicity and surface roughness are major factors that impact the membrane's antifouling properties.[12,13,19,46,55,56]

Typically, studies report that hydrophilic surfaces that have low surface roughness are less prone to fouling. This assumption is reasonable because if the membrane is more hydrophobic, hydrophobic organic molecules will interact more with the membrane's surface, which facilitates surface contamination.[12] Similarly, increasing roughness can have a negative impact on the antifouling properties because foulants, like proteins, are more likely to be adsorbed in the valleys of the membrane, and as such, there is a greater surface area to which foulants can be attached.[19,46] In this study, the sulfidized membranes are more hydrophilic but show an increase in surface roughness. The overall fouling propensity of a surface is difficult to predict, even after the individual assessment of the surface properties. Therefore, dynamic bacteria deposition assays were done to elucidate which membrane will have the highest fouling resistance.

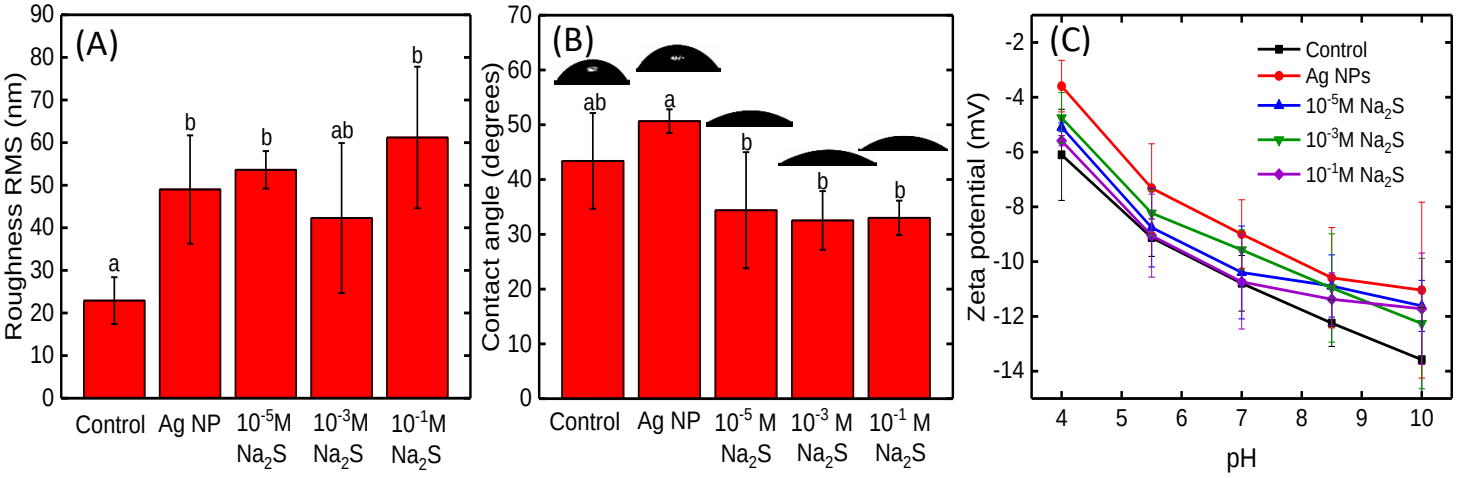

Figure 2. Membrane surface properties of control and functionalized membranes. (A) Surface roughness (root mean square) measured by AFM (B) CA measured by surface contact angles, and (C) zeta potential measured at acidic, neutral, and basic pHs. Different letters indicate statistical difference ($p < 0.05$).

3.3 Sulfidation slows down silver leaching. An important question in this work concerns how sulfidation affects the Ag NPs behavior in natural systems. Ag NPs dissolve in aqueous solutions and release silver ions (Ag^+). Although this property is expected and desirable for biofouling control, the continuous dissolution of Ag NPs reduces the antifouling efficacy of the membrane during use and adds to the cost of membrane operation.[39] Furthermore, the release of silver into concentrated brines is an additional challenge to consider. In this study, silver sulfidation is proposed as a mean to extend the service life of Ag NP-enabled membranes and control silver release.

The release of Ag^+ is an important parameter to consider for risk assessment as it relates to the toxicity imparted by Ag NPs. Figure 3 shows the Ag^+ release rate of the functionalized membranes according to their sulfur to silver (S/Ag) ratio. The silver remaining on each membrane after each time interval (0-6h) is shown in Figure S2. The

silver membrane (no sulfur) has a Ag^{+} release rate of 157.5 ± 54.9 ng/ cm^2-hr whereas the sulfidized membranes have a release rate of 80.9 ± 57.1, 31.9 ± 37.7, and 20.6 ± 16.9 for the 10^{-5}M Na_2S, 10^{-3}M Na_2S, and 10^{-1}M Na_2S respectively. This trend suggests that the sulfidation of Ag NPs can decrease by > 85% the mass of silver released depending on the sulfidizing agent's concentration, as similarly observed in previous studies[48,57] The sulfidation of metals influence their toxicity in natural environments due to the low solubility of metal sulfide species; the decrease in silver release after sulfidation is consistent with the low solubility constant for Ag_2S ($K_{sp} = 10^{-50}$).[32,58]

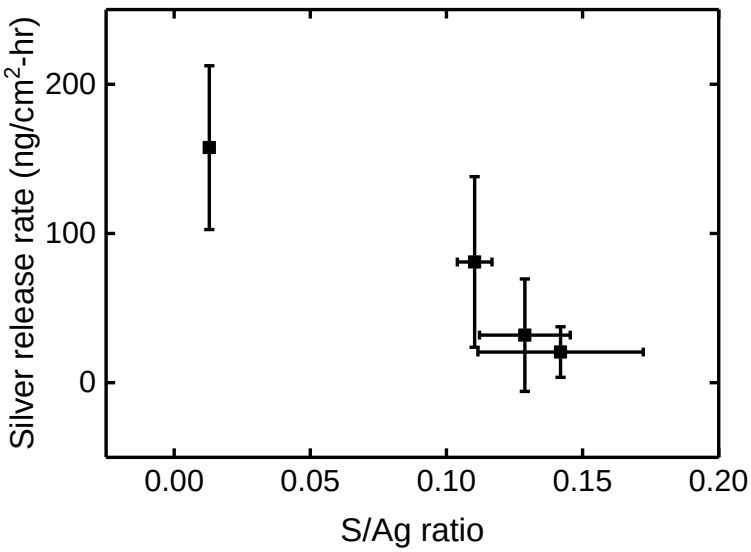

Figure 3. Effect of sulfidation (S/Ag ratio) on the silver release from the membrane. Silver release was calculated based on the silver remaining on the membrane over time, after acid digestion, by ICP-MS.

3.4 Sulfidation preserves the antibacterial activity. The antibacterial properties of silver ions are attributed to three main mechanisms: i) Interaction with sulfhydryl groups on the cell surface, which may block respiration and electron transfer to lead to the de-energizing of the membrane and cell death; ii) A small ionic radius (0.115 nm) allowing Ag ions to travel through transmembrane proteins like porins (1-3 nm) and react with thiol functional groups in proteins and nucleic acids, which interfere with DNA replication or deactivate multiple enzymes; and iii) Increase ROS levels due to the deactivation of thiol-containing and antioxidative enzymes.[29,59] Ag NPs are efficient antibacterial agent because they exhibit enhanced silver ion release per unit mass due to an increased surface area to volume ratio.

Even though Ag NPs can offer strong antibacterial properties, their rapid dissolution in aqueous matrices limits their applications and promotes a faster release into the environment. Sulfidation of Ag NPs is a promising technique to maintain the efficiency of Ag NPs' toxicity while slowing down silver release. Viability of *P. aeruginosa* and *E. coli* was measured via CFU counts by exposing functionalized coupons to a bacteria solution for 3h. *E. coli* was used due to its widespread use as a model for the testing of antimicrobial surfaces. Figure 4 results show a significant CFU reduction for both bacteria. *P. aeruginosa*, a model biofilm bacterium, reduced cell viability to 39.5 ± 17.2, 26.9 ± 12.6, 44.0 ± 20.3, and 55.7 ± 23.7% for coupons functionalized with Ag NPs, 10^{-5}, 10^{-3}, and 10^{-1} M Na_2S. Similar results were observed with *E. coli*, where cell viability reduced to 50.0 ± 20.4% when exposed to coupons functionalized with Ag NPs and to 48.5 ± 19.1, 42.9 ± 15.1, and 75.4 ± 32.5%, for coupons coated with 10^{-5}, 10^{-3}, and 10^{-1} M Na_2S, respectively, compared to the control. The highest antibacterial activity for *P. aeruginosa* was achieved with the 10^{-5} M Na_2S coupon, where cell viability reduced by 73% whereas for *E. coli* viability was lowest at 57% after exposure to 10^{-3} M Na_2S. These results indicate that *P. aeruginosa* has a higher sensitivity to silver compared to *E. coli*, as observed in a similar study by Ben-Sasson et al.[22] In both bacterial assays, both Ag NP-coated and sulfidized membranes reduced cell viability in a statistically significant way except for the most sulfidized membrane (10^{-1} M Na_2S) which was not statistically different from the control. However, there is no statistical difference between the Ag NP-functionalized and sulfidized membranes. Based on these results and in agreeance with Levard et al.[48], we observe a threshold of Ag NP sulfidation where the antibacterial activity is reduced.

Similar results have been observed in the literature, where Ag NPs decrease cell viability in *P. aeruginosa*[18,56] and Ag NP sulfidation decreases toxicity towards *E. coli*,[47] nitrifying bacteria,[60] and *C. elegans*.[61] Reinsch et al.[47] observed that higher Ag_2S/Ag^0 ratio resulted in less growth inhibition of *E. coli* over 6h of exposure. Devi et al.[62] observed that Ag NPs enhanced oxidative stress whereas Ag NP sulfidation alleviated changes in oxidative stress, detoxification enzymes and brain acetylcholinesterase activity in adult

zebrafish. All of these findings were attributed to the lower solubility of Ag_2S compared to Ag^0 NPs.

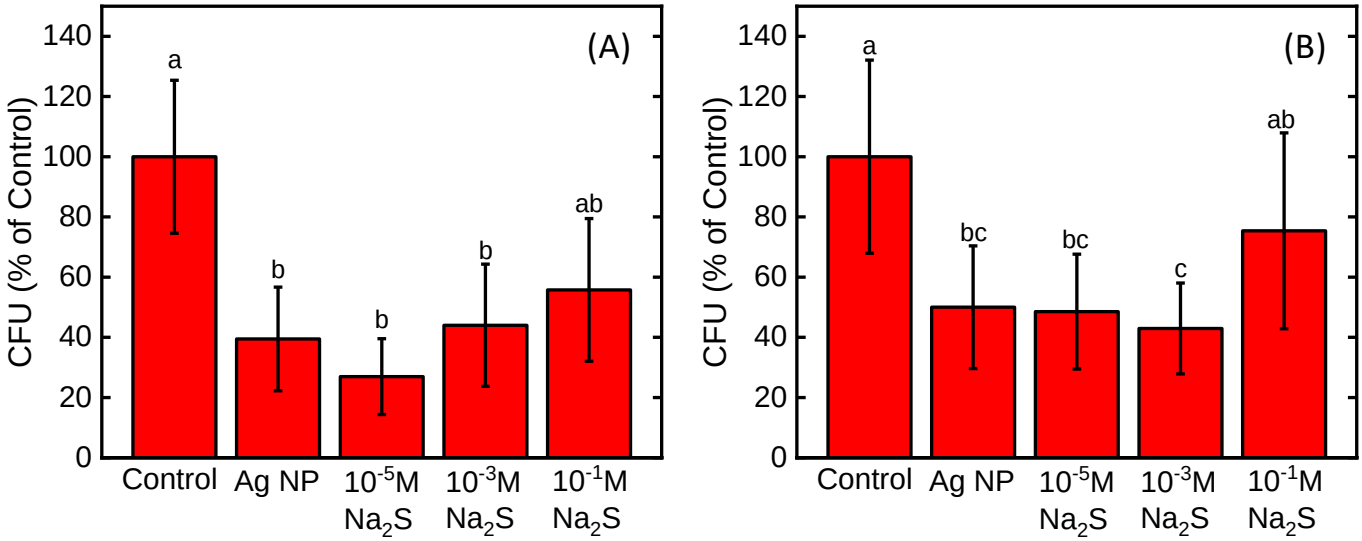

Figure 4. Number of viable colony forming units (CFU) on a 4.9 cm^2 coupon after 3h of contact with 10^7 CFU/mL of (A) *P. aeruginosa* and (B) *E. coli*. Results have been normalized with respect to the control. Different letters indicate statistical difference ($p < 0.05$). n=9.

3.5 Biofouling experiments and residual silver after biofouling. To determine the biofouling mitigation potential of functionalized membranes, a set of experiments using a bench-scale RO fouling system were done using a synthetic secondary wastewater spiked with *P. aeruginosa*. This bacterium was chosen as a model organism for membrane biofouling studies due to its biofilm forming ability.[63] Additionally, this bacterium produces at least three extracellular polysaccharides, which are a constituent of EPS which in turn have been suggested to be the predominant culprit for biofouling of RO membranes.[7,8] Over a course of 24h, a gradual decline in the permeate flux was observed due to biofilm development for all samples (Figure 5A). The control membrane had a flux decline of 29% ± 0.8. When compared to the control membrane, the Ag NPs, and all sulfidized membranes (10^{-5} M, 10^{-3} M, and 10^{-1} M Na_2S) resulted in a significantly lower permeate flux decline with a 24% ± 0.7, 23% ± 1, 17% ± 2, and 19% ± 1 decline, respectively (Figure 5B). Silver functionalization and further sulfidation was able to reduce the effect of biofouling under dynamic biofouling conditions. Even though there is less silver being released from the sulfidized membranes, the toxicity of the Ag NPs and Ag ions led to a reduction of live bacteria on the membrane, consequently leading to an increased fouling resistance.[22,56] This can be attributed to the fact that very low doses of

Ag are required to impart a biocidal effect. Additionally, the sulfidized membranes have more silver remaining which leads to more silver released over longer periods of time and thus, prevent bacterial attachment. This effect is better observed with the 10^{-1}M Na_2S membrane, where the slower release of Ag^+ is sufficient to impart biofouling resistance.

Residual silver was measured to assess the Ag^+ release potential after biofouling (Figure 5C). In agreement with the release rates discussed above, it is observed that the sulfidized membranes with the highest S/Ag ratio retain more silver than the Ag NPs. The 10^{-1} M Na_2S membrane had 519 ± 209 ng/cm^2 of Ag compared to 132 ± 209 ng/cm^2 from the Ag NPs membrane. These results show that sulfidation is a promising technique for membrane technologies: it slows down silver release, while retaining the Ag NPs biocidal properties. More importantly, these results highlight that silver retention on the surface is more important for biofouling resistance than biocidal properties measured under static conditions.

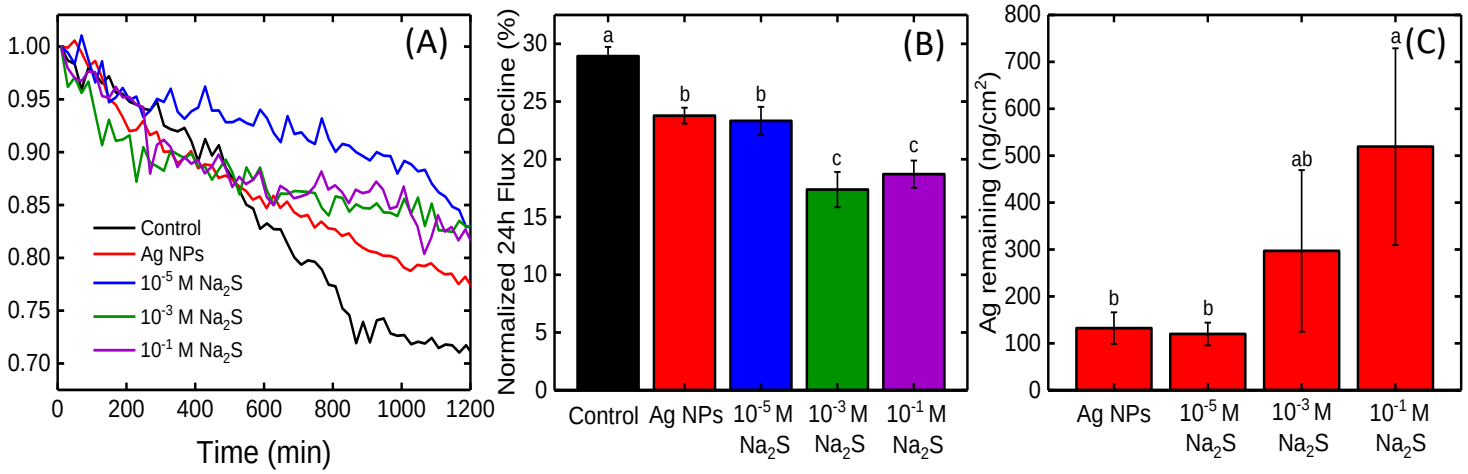

Figure 5. (A) Normalized average flux decline over 24h of RO modules tested with the control and each of the functionalized membranes. The initial *P. aeruginosa* concentration in the synthetic secondary wastewater medium was 2.5 × 10^6 cells/mL. (B) Normalized flux decline of each bench-scale RO run (n=3). The final permeate flux was calculated from the average of the flux for the last 20 min of the experiment. (C) Ag remaining after 24 h of RO modules tested with the control and each of the functionalized membranes. Ag was quantified using ICP-MS. Different letters indicate statistical difference ($p < 0.05$) n=9.

4. Conclusions

Biocidal coatings using silver have been shown to impart biofouling control on membranes. However, one of the main drawbacks of silver is its rapid ion release and eventual depletion from the membrane, which affect its performance and antibacterial activity. This study provides insights into how sulfidation of Ag NPs can overcome the aforementioned barriers. Different extents of sulfidation were studied to assess the antibacterial activity,

silver release and biofouling resistance of the *in situ* Ag:Ag_2S particles. Sulfidation of Ag NPs can decrease silver release by > 85% without affecting the antibacterial activity, however, there is a threshold of sulfidation where the antibacterial activity can be lost. In addition, this study demonstrates that static biocidal performance does not predict biofouling resistance and that even for the sulfidized Ag:Ag_2S particles showing reduced antibacterial activity, high biofouling resistance is observed due to the higher retention of silver on the membrane surface. Overall, sulfidation is a simple and effective way to prolong the lifetime of anti-biofouling Ag NP coatings. Future research should focus at testing the membrane performance for longer periods of time and under real water conditions to evaluate the effect of the complex water matrix in natural waters.

Acknowledgements

This work was supported the National Science Foundation, through the Nanosystems Engineering Research Center for Nanotechnology-Enabled Water Treatment (EEC-1449500), and the NASA STTR program (contract no. 80NSSC19C0566). We acknowledge the contribution of Naiara Mottim Justino for her assistance in the membrane performance characterization. A.B. acknowledges the support of a Dean's Fellowship from the Ira A. Fulton Schools of Engineering and a Scholar Award given by the International Chapter of the P.E.O. Sisterhood. We acknowledge the use of TEM facilities within the Eyring Materials Center at Arizona State University supported in part by NNCI-ECCS-1542160.

References

1 A. Y. Hoekstra, M. M. Mekonnen, A. K. Chapagain, R. E. Mathews and B. D. Richter, Global monthly water scarcity: Blue water footprints versus blue water availability, *PLoS One*, 2012, **7**, e32688.

2 M. Elimelech and W. A. Phillip, The Future of Seawater Desalination: Energy, Technology, and the Environment, *Science*, 2011, **333**, 712–717.

3 J. R. Werber, C. O. Osuji and M. Elimelech, Materials for next-generation desalination and water purification membranes, *Nat. Rev. Mater.*, 2016, **1**, 16018.

4 G. Amy, N. Ghaffour, Z. Li, L. Francis, R. Valladares, T. Missimer and S. Lattemann, Membrane-based seawater desalination : Present and future prospects, *Desalination*, 2017, **401**, 16–21.

5 J. S. Baker and L. Y. Dudley, Biofouling in membrane systems — A review, *Desalination*, 1998, **118**, 81–89.

6 C. Dreszer, H. C. Flemming, A. Zwijnenburg, J. C. Kruithof and J. S. Vrouwenvelder, Impact of biofilm accumulation on transmembrane and feed channel pressure drop: Effects of crossflow velocity, feed spacer and biodegradable nutrient, *Water Res.*, 2014, **50**, 200–211.

7 M. Herzberg and M. Elimelech, Biofouling of reverse osmosis membranes: Role of biofilm-enhanced osmotic pressure, *J. Memb. Sci.*, 2007, **295**, 11–20.

8 H. Flemming, Reverse Osmosis Membrane Biofouling, *Exp. Therm. Fluid Sci.*, 1997, **14**, 382–391.

9 S. S. Madaeni, T. Mohamamdi and M. K. Moghadam, Chemical cleaning of reverse osmosis membranes, *Desalination*, 2001, **134**, 77–82.

10 F. Ridgeway, Harry, *Biological fouling of separation membranes used in water treatment applications*, AWWA Research Foundation, 2003.

11 V. Kochkodan and N. Hilal, A comprehensive review on surface modified polymer membranes for biofouling mitigation, *Desalination*, 2015, **356**, 187–207.

12 D. Rana and T. Matsuura, Surface modifications for antifouling membranes., *Chem. Rev.*, 2010, **110**, 2448–71.

13 A. Bogler, S. Lin and E. Bar-Zeev, Biofouling of membrane distillation, forward osmosis and pressure retarded osmosis: Principles, impacts and future directions, *J. Memb. Sci.*, 2017, **542**, 378–398.

14 M. R. Hibbs, L. K. McGrath, S. Kang, A. Adout, S. J. Altman, M. Elimelech and C. J. Cornelius, Designing a biocidal reverse osmosis membrane coating: Synthesis and biofouling properties, *Desalination*, 2016, **380**, 52–59.

15 N. Akar, B. Asar, N. Dizge and I. Koyuncu, Investigation of characterization and biofouling properties of PES membrane containing selenium and copper nanoparticles, *J. Memb. Sci.*, 2013, **437**, 216–226.

16 A. Inurria, P. Cay-Durgun, D. Rice, H. Zhang, D. K. D.-K. Seo, M. L. Lind and F. Perreault, Polyamide thin-film nanocomposite membranes with graphene oxide nanosheets: Balancing membrane performance and fouling propensity, *Desalination*, 2019, **451**, 139–147.

17 G. Ye, J. Lee, F. Perreault and M. Elimelech, Controlled Architecture of Dual-Functional Block Copolymer Brushes on Thin-Film Composite Membranes for Integrated ‘defending’ and ‘attacking’ Strategies against Biofouling, *ACS Appl. Mater. Interfaces*, 2015, **7**, 23069–23079.

18 M. Ben-Sasson, K. R. Zodrow, Q. Genggeng, Y. Kang, E. P. Giannelis and M. Elimelech, Surface functionalization of thin-film composite membranes with copper nanoparticles for antimicrobial surface properties, *Environ. Sci. Technol.*, 2014, **48**, 384–393.

19 M. S. Rahaman, H. Thérien-Aubin, M. Ben-Sasson, C. K. Ober, M. Nielsen and M. Elimelech, Control of biofouling on reverse osmosis polyamide membranes modified with biocidal nanoparticles and antifouling polymer brushes, *J. Mater. Chem. B*, 2014, **2**, 1724–1732.

20 A. Soroush, W. Ma, Y. Silvino and M. S. Rahaman, Surface modification of thin film composite forward osmosis membrane by silver-decorated graphene-oxide nanosheets, *Environ. Sci. Nano*, 2015, **2**, 395–405.

21 A. Soroush, W. Ma, M. Cyr, M. S. Rahaman, B. Asadishad and N. Tufenkji, In Situ Silver Decoration on Graphene Oxide-Treated Thin Film Composite Forward Osmosis Membranes: Biocidal Properties and Regeneration Potential, *Environ. Sci. Technol. Lett.*, 2016, **3**, 13–18.

22 M. Ben-Sasson, X. Lu, E. Bar-Zeev, K. R. Zodrow, S. Nejati, G. Qi, E. P. Giannelis and M. Elimelech, In situ formation of silver nanoparticles on thin-film composite reverse osmosis membranes for biofouling mitigation, *Water Res.*, 2014, **62**, 260–270.

23 A. F. Faria, C. Liu, M. Xie, F. Perreault, L. D. Nghiem, J. Ma and M. Elimelech, Thin-film composite forward osmosis membranes functionalized with graphene oxide–silver nanocomposites for biofouling control, *J. Memb. Sci.*, 2017, **525**, 146–156.

24 J. Yin, Y. Yang, Z. Hu and B. Deng, Attachment of silver nanoparticles (AgNPs) onto thin-film composite (TFC) membranes through covalent bonding to reduce membrane biofouling, *J. Memb. Sci.*, 2013, **441**, 73–82.

25 K. Zodrow, L. Brunet, S. Mahendra, D. Li, A. Zhang, Q. Li and P. J. J. Alvarez, Polysulfone ultrafiltration membranes impregnated with silver nanoparticles show improved biofouling resistance and virus removal, *Water Res.*, 2009, **43**, 715–723.

26 A. Zirehpour, A. Rahimpour, A. Arabi Shamsabadi, M. G. Sharifian and M. Soroush, Mitigation of Thin-Film Composite Membrane Biofouling via Immobilizing Nano-Sized Biocidal Reservoirs in the Membrane Active Layer, *Environ. Sci. Technol.*, 2017, **51**, 5511–5522.

27 S. Prabhu and E. K. Poulose, Silver nanoparticles : mechanism of antimicrobial action , synthesis , medical applications , and toxicity effects, *Int. Nano Lett.*, 2012, **2**, 1–10.

28 I. Kurvet, A. Kahru, O. Bondarenko, A. Ivask and A. Ka, Particle-Cell Contact Enhances Antibacterial Activity of Silver Nanoparticles, *PLoS One*, 2013, **8**, e64060.

29 L. M. Stabryla, K. A. Johnston, J. E. Millstone and L. M. Gilbertson, Emerging investigator series: It's not all about the ion: Support for particle-specific contributions to silver nanoparticle antimicrobial activity, *Environ. Sci. Nano*, 2018, **5**, 2047–2068.

30 W. Li, X. Xie and Q. Shi, Antibacterial activity and mechanism of silver nanoparticles on Escherichia coli, *Appl. Microbiol. Biotechnol.*, 2010, **85**, 1115–1122.

31 Z. M. Xiu, Q. B. Zhang, H. L. Puppala, V. L. Colvin and P. J. J. Alvarez, Negligible particle-specific antibacterial activity of silver nanoparticles, *Nano Lett.*, 2012, **12**, 4271–4275.

32 C. C. Levard, E. M. Hotze, G. V. Lowry and G. E. Brown, Environmental Transformations of Silver Nanoparticles: Impact on Stability and Toxicity, *Environ. Sci. Technol.*, 2012, **46**, 6900–6914.

33 J. Liu, D. a Sonshine, S. Shervani and R. H. Hurt, Controlled Release of Biologically Active Silver from Nanosilver Surfaces, *ACS Nano*, 2010, **4**, 6903–6913.

34 A. F. De Faria, D. S. T. Martinez, S. M. M. Meira, A. C. M. de Moraes, A. Brandelli, A. G. S. Filho and O. L. Alves, Anti-adhesion and antibacterial activity of silver nanoparticles supported on graphene oxide sheets, *Colloids Surfaces B Biointerfaces*, 2014, **113**, 115–124.

35 L. Tang, K. J. T. Livi and K. L. Chen, Polysulfone membranes modified with bioinspired polydopamine and silver nanoparticles formed in situ to mitigate biofouling, *Environ. Sci. Technol. Lett.*, 2015, **2**, 59–65.

36 Z. Liu and Y. Hu, Sustainable Antibiofouling Properties of Thin Film Composite Forward Osmosis Membrane with Rechargeable Silver Nanoparticles Loading, *ACS Appl. Mater. Interfaces*, 2016, **8**, 21666–21673.

37 L. Qi, Y. Hu, Z. Liu, X. An and E. Bar-Zeev, Improved Anti-Biofouling Performance of Thin -Film Composite Forward-Osmosis Membranes Containing Passive and Active Moieties, *Environ. Sci. Technol.*, 2018, **52**, 9684–9693.

38 Z. Liu, L. Qi, X. An, C. Liu and Y. Hu, Surface Engineering of Thin Film Composite Polyamide Membranes with Silver Nanoparticles through Layer-by-Layer Interfacial Polymerization for Antibacterial Properties, *ACS Appl. Mater. Interfaces*, 2017, **9**, 40987–40997.

39 Y. Bi, B. Han, S. Zimmerman, F. Perreault, S. Sinha and P. Westerhoff, Four release tests exhibit variable silver stability from nanoparticle-modified reverse osmosis membranes, *Water Res.*, 2018, **143**, 77–86.

40 P. Glueckstern, M. Priel, E. Gelman and N. Perlov, Wastewater desalination in Israel, *Desalination*, 2008, **222**, 151–164.

41 M. D. Johnston, E. A. Simons and R. J. W. Lambert, One explanation for the variability of the bacterial suspension test, *J. Appl. Microbiol.*, 2000, **88**, 237–242.

42 K. P. Koutsoumanis and A. Lianou, Stochasticity in colonial growth dynamics of individual bacterial cells, *Appl. Environ. Microbiol.*, 2013, **79**, 2294–2301.

43 Z. Aspridou and K. P. Koutsoumanis, Individual cell heterogeneity as variability source in population dynamics of microbial inactivation, *Food Microbiol.*, 2015, **45**, 216–221.

44 J. A. Brant, K. M. Johnson and A. E. Childress, Characterizing NF and RO membrane surface heterogeneity using chemical force microscopy, *Colloids Surfaces A Physicochem. Eng. Asp.*, 2006, **280**, 45–57.

45 Y. Kim, S. Lee, J. Kuk and S. Hong, Surface chemical heterogeneity of polyamide RO membranes: Measurements and implications, *Desalination*, 2015, **367**, 154–160.

46 E. M. V. Hoek, S. Bhattacharjee and M. Elimelech, Effect of membrane surface roughness on colloid-membrane DLVO interactions, *Langmuir*, 2003, **19**, 4836–4847.

47 B. C. Reinsch, C. Levard, Z. Li, R. Ma, A. Wise, K. B. Gregory, G. E. Brown and G. V. Lowry, Sulfidation of silver nanoparticles decreases Escherichia coli growth inhibition, *Environ. Sci. Technol.*, 2012, **46**, 6992–7000.

48 C. Levard, B. C. Reinsch, F. M. Michel, C. Oumahi, G. V. Lowry and G. E. Brown, Sulfidation processes of PVP-coated silver nanoparticles in aqueous solution: Impact on dissolution rate, *Environ. Sci. Technol.*, 2011, **45**, 5260–5266.

49 M. Pang, J. Hu and H. C. Zeng, Synthesis, morphological control, and antibacterial properties of hollow/solid Ag2S/Ag heterodimers, *J. Am. Chem. Soc.*, 2010, **132**, 10771–10785.

50 S. M. Magaña, P. Quintana, D. H. Aguilar, J. A. Toledo, C. Ángeles-Chávez, M. A. Cortés, L. León, Y. Freile-Pelegrín, T. López and R. M. T. Sánchez, Antibacterial activity of montmorillonites modified with silver, *J. Mol. Catal. A Chem.*, 2008, **281**, 192–199.

51 L. Li, Y. Wang, Q. Liu and G. Jiang, Rethinking Stability of Silver Sulfide Nanoparticles (Ag2S-NPs) in the Aquatic Environment: Photoinduced Transformation of Ag2S-NPs in the Presence of Fe(III), *Environ. Sci. Technol.*, 2016, **50**, 188–196.

52 G. Goncalves, P. A. A. P. Marques, C. M. Granadeiro, H. I. S. Nogueira, M. K. Singh and J. Grácio, Surface modification of graphene nanosheets with gold nanoparticles: The role of oxygen moieties at graphene surface on gold nucleation and growth, *Chem. Mater.*, 2009, **21**, 4796–4802.

53 K. Spilarewicz-Stanek, A. Kisielewska, J. Ginter, K. Bałuszyńska and I. Piwoński, Elucidation of the function of oxygen moieties on graphene oxide and reduced graphene oxide in the nucleation and growth of silver nanoparticles, *RSC Adv.*, 2016, **6**, 60056–60067.

54 K. P. Lee, T. C. Arnot and D. Mattia, A review of reverse osmosis membrane materials for desalination-Development to date and future potential, *J. Memb. Sci.*, 2011, **370**, 1–22.

55 E. M. Vrijenhoek, S. Hong and M. Elimelech, Influence of membrane surface

properties on initial rate of colloidal fouling of reverse osmosis and nanofiltration membranes, *J. Memb. Sci.*, 2001, **188**, 115–128.

56 D. Rice, A. C. A. C. Barrios, Z. Xiao, A. Bogler, E. Bar-Zeev and F. Perreault, Development of anti-biofouling feed spacers to improve performance of reverse osmosis modules, *Water Res.*, 2018, **145**, 599–607.

57 S. W. Lee, S. Y. Park, Y. Kim, H. Im and J. Choi, Effect of sulfidation and dissolved organic matters on toxicity of silver nanoparticles in sediment dwelling organism, Chironomus riparius, *Sci. Total Environ.*, 2016, **553**, 565–573.

58 D. Ma, X. Hu, H. Zhou, J. Zhang and Y. Qian, Shape-controlled synthesis and formation mechanism of nanoparticles-assembled Ag2S nanorods and nanotubes, *J. Cryst. Growth*, 2007, **304**, 163–168.

59 C. Levard, E. M. Hotze, B. P. Colman, A. L. Dale, L. Truong, X. Y. Yang, A. J. Bone, G. E. Brown, R. L. Tanguay, R. T. Di Giulio, E. S. Bernhardt, J. N. Meyer, M. R. Wiesner and G. V. Lowry, Sulfidation of silver nanoparticles: Natural antidote to their toxicity, *Environ. Sci. Technol.*, 2013, **47**, 13440–13448.

60 O. Choi, T. E. Clevenger, B. Deng, R. Y. Surampalli, L. Ross and Z. Hu, Role of sulfide and ligand strength in controlling nanosilver toxicity, *Water Res.*, 2009, **43**, 1879–1886.

61 D. L. Starnes, J. M. Unrine, C. P. Starnes, B. E. Collin, E. K. Oostveen, R. Ma, G. V. Lowry, P. M. Bertsch and O. V. Tsyusko, Impact of sulfidation on the bioavailability and toxicity of silver nanoparticles to Caenorhabditis elegans, *Environ. Pollut.*, 2015, **196**, 239–246.

62 G. P. Devi, K. B. A. Ahmed, M. K. N. S. Varsha, B. S. Shrijha, K. K. S. Lal, V. Anbazhagan and R. Thiagarajan, Sulfidation of silver nanoparticle reduces its toxicity in zebrafish, *Aquat. Toxicol.*, 2015, **158**, 149–156.

63 R. J. Barnes, R. R. Bandi, F. Chua, J. Hui, T. Aung, N. Barraud, A. G. Fane, S. Kjelleberg and S. A. Rice, The roles of Pseudomonas aeruginosa extracellular polysaccharides in biofouling of reverse osmosis membranes and nitric oxide induced dispersal, *J. Memb. Sci.*, 2014, **466**, 161–172.

Graphical Abstract

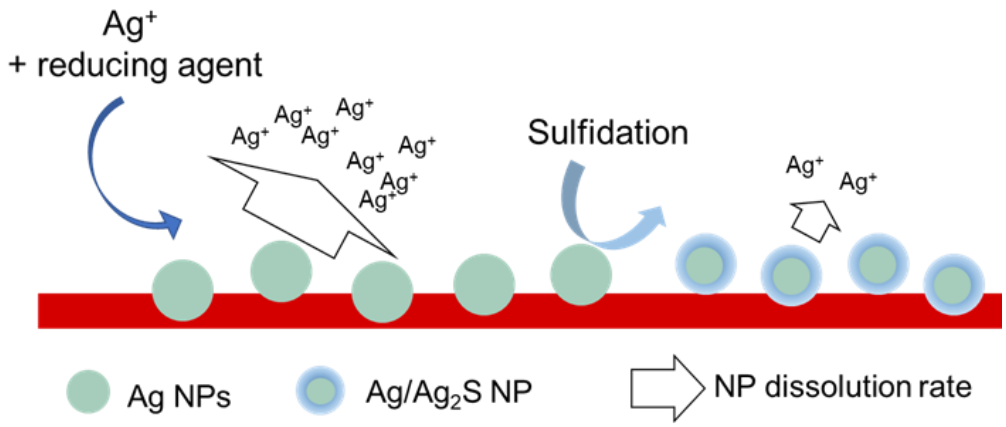

Novelty statement: Silver sulfidation in nanosilver-coated membranes slows down silver release and increase biofouling resistance without affecting the membrane's functionality